A Non-Invasive Blood Pressure Estimation Method Based on Mamba-UNet and PPG Signals

1st Huiqun Yu Shanghai University of Electric Power Shanghai, China yuhuiqun@shiep.edu.cn 2nd Haonan Fan Shanghai University of Electric Power Shanghai, China 2485672461@qq.com 3rd Qingde Li University of Hull Hull, United Kingdom Q.Li@hull.ac.uk

4th Fangfang Lu*
Shanghai University of Electric Power
Shanghai, China
lufangfang@shiep.edu.cn*

5th Yongqiang Cheng University of Sunderland Sunderland, United Kingdom Yongqiang.Cheng@sunderland.ac.uk

Abstract—Continuous blood pressure monitoring is of great significance for the early diagnosis of cardiovascular diseases. To address the limitations of current machine learning and deep learning-based blood pressure (BP) prediction methods, which rely on manual feature extraction and struggle to reconstruct complete BP waveforms, this paper employs a continuous noninvasive arterial BP detection model named Mamba-UNet based on photoplethysmography (PPG) signals. The model deeply integrates the selective state space model (Selective SSM) with the U-Net architecture, achieving direct mapping from PPG signals to arterial blood pressure (ABP) waveforms through end-to-end modeling. In the encoder, the MambaConvBlock module captures long-term temporal dependencies and individual vascular characteristics of PPG signals by dynamically adjusting parameters (Δ, B, C) . The decoder employs a hybrid Mamba-convolution structure, combining the global dynamic modeling capability of SSM with the local feature extraction ability of convolution to accurately reconstruct BP waveform details. The model design balances the multi-scale feature integration advantages of U-Net with the efficient long-sequence processing capability of Mamba. Evaluated on the Sensors dataset (derived from MIMIC-III. containing 1,131 ICU patient records), Mamba-UNet achieved a mean absolute error (MAE) of 6.06 mmHg for diastolic blood pressure (DBP) and 13.11 mmHg for systolic blood pressure (SBP), outperforming models such as MLP, ResNet, and U-Net.

Index Terms—Arterial blood pressure (ABP), photoplethysmography (PPG), Mamba, U-Net, non-invasive.

I. Introduction

Cardiovascular diseases are one of the leading causes of death worldwide, with the incidence continuing to rise. These diseases are increasingly affecting younger populations and exhibiting a trend of diverse risk factors [1]. Hypertension, as one of the most important independent risk factors for cardiovascular diseases, is closely related to coronary heart disease, stroke, heart failure, and other cardiovascular conditions [2]. Accurate and continuous blood pressure (BP) monitoring is essential for the early detection of hypertension and abnormal BP fluctuations, as well as for guiding disease prevention, diagnosis, and personalized treatment. It is a key aspect in controlling the occurrence and progression of cardiovascular diseases [3].

Currently, the commonly used BP measurement tools in hospitals and homes are the mercury sphygmomanometer and the electronic cuff-based BP monitor. These methods provide relatively accurate results, but the cuff inflation process can cause discomfort or even stress reactions in some individuals, which may affect the true accuracy of the measurements. To address these problems, cuffless BP measurement technologies have been developed. These methods assess BP without the use of an inflatable cuff. The advantages include greater comfort, reduced measurement errors caused by stress reactions, and the ability to enable non-invasive continuous monitoring, making them a promising option for both clinical and home use.

Early cuffless blood pressure measurement methods primarily included techniques based on pulse transit time (PTT), arterial volume change detection (such as piezoelectric or pressure sensors), and arterial acoustic or vibration signal analysis [4]. In recent years, researchers have extensively explored the application of various machine learning methods in blood pressure prediction. Zhang et al. [5] applied the classification and regression tree (CART) model to model blood pressure, [6] introduced the support vector regression (SVR) algorithm to achieve blood pressure estimation based on physiological indicators, and [7] further used the gradient boosting decision tree (GBDT) to build a continuous blood pressure prediction model, showing higher prediction accuracy. These methods offer advantages such as non-invasiveness, wearability, and the convenience of continuous monitoring, and were widely explored as potential replacements for traditional cuff-based blood pressure monitors [8]. However, these approaches face several limitations. For instance, the PTT method is highly affected by individual differences, requires initial calibration, and is very sensitive to posture and movement, sensor-based methods for detecting arterial deformation have high requirements for sensor placement and are prone to drift and noise interference, while audio and vibration analysis methods have non-contact potential, the signals are weak, easily drowned out by environmental noise, and the measurement accuracy still needs improvement.

Compared with traditional cuffless BP methods, photoplethysmography (PPG)-based BP prediction offers advantages in convenience and suitability for continuous monitoring. It does not require pressure application, resulting in greater comfort and suitability for frequent or long-term measurements. PPG signals are easy to acquire and can be integrated into wearable devices for real-time, around-the-clock monitoring, providing a better reflection of dynamic blood pressure changes [9]. Current approaches mainly include feature engineering combined with traditional machine learning, and end-to-end deep learning models [10]. The former is highly interpretable and easy to implement, but relies on manual expertise and has limited generalizability, the latter can automatically learn complex patterns from raw signals, making it suitable for large-scale data modeling, and has attracted considerable research interest in recent years.

With the advancement of deep learning, increasing attention has been given to the use of raw PPG signals for non-invasive and continuous BP monitoring. Convolutional neural networks (CNN) and long short-term memory (LSTM) networks are widely used for feature extraction and temporal modeling. The CNN-LSTM model proposed in [11] was evaluated on the MIMIC II database, and its results met the AAMI standards and achieved Grade A according to the BHS standard. In [12], LeNet-5 and U-Net autoencoders were compared, with genetic algorithms applied to optimize their integration. The model performed excellently in blood pressure estimation, with mean absolute error (MAE) values of 2.54 mmHg for systolic blood pressure (SBP) and 1.48 mmHg for diastolic blood pressure (DBP). The Spectrotemporal ResNet model proposed in [13] was validated on 510 participants from the MIMIC III database, and achieved MAE values of 9.43 mmHg for SBP and 6.88 mmHg for DBP. Although the PPG method offers advantages in convenience and non-invasiveness, challenges remain regarding prediction accuracy and generalization ability, requiring further optimization.

In this paper, a model named Mamba-UNet is applied, which innovatively integrates the selective state space model (Selective SSM) with the U-Net architecture, specifically designed for non-invasive continuous blood pressure prediction using PPG signals. The core contributions of Mamba-UNet include employing MambaConvBlock in the encoder to dynamically capture long-range dependencies and individual vascular differences in PPG signals, and utilizing a hybrid Mamba-convolution module in the decoder to accurately reconstruct blood pressure waveforms. The incorporation of a selective mechanism allows parameters Δ , B, and C to dynamically adapt to the input, effectively suppressing motion artifact interference. Combined with hardware-aware optimizations such as kernel fusion and parallel scanning, the model enables efficient processing of million-scale sequences, achieving five times the inference throughput compared to Transformer-based approaches [14]. Its end-to-end architecture directly outputs continuous blood pressure waveforms and key parameters (systolic/diastolic pressure), while the decoder's multi-level feature maps enhance clinical interpretability. This model addresses key limitations of traditional methods, such as reliance on calibration and inefficiency in long-sequence processing, offering a high-precision, robust deep learning solution for real-time, non-invasive blood pressure monitoring with significant clinical application potential.

The rest of this paper is organized as follows: Section II provides a detailed description of the methodology used in this study, including the dataset, data preprocessing procedures, and the employed model architecture. Section III presents the experimental results, covering the experimental setup and comparisons with other methods. Section IV concludes the paper.

TABLE I LIST OF ABBREVIATIONS AND NOMENCLATURE

Abbreviation	Full Term or Meaning		
BP	Blood Pressure		
PPG	Photoplethysmography		
Selective SSM	selective state space model		
ABP	arterial blood pressure		
PTT	pulse transit time		
SVR	support vector regression		
GBDT	gradient boosting decision tree		
CNN	Convolutional Neural Network		
LSTM	Long Short-Term Memory		
MAE	mean absolute error		
SBP	systolic blood pressure		
DBP	diastolic blood pressure		
ICU	intensive care unit		
MSE	mean squared error		
ME	mean error		
BHS	British Hypertension Society		

II. METHODOLOGY

A. Data Collection

As shown in Table I, the key abbreviations and their full definitions used throughout this paper are summarized for reference. In this paper, the Sensors dataset was utilized, which is a subset extracted from the MIMIC-III database and contains records from 1,131 patients in the intensive care unit (ICU) [15]. This dataset includes high-quality PPG and corresponding arterial blood pressure (ABP) signals from the MIMIC-III database, forming input-target signal pairs commonly used in BP estimation research. Unlike traditional continuous signal datasets, the Sensors dataset adopts a discrete sampling strategy by retaining only two 15-second waveform segments per patient, sampled 5 minutes apart. This approach ensures signal diversity while maintaining a manageable dataset size. The dataset features a medium-to-large sample scale, high interindividual variability, a reasonable distribution of waveform segments, and good data standardization. This makes it wellsuited for training and evaluating deep learning models for BP estimation, particularly for assessing model generalization and capturing short-term physiological dynamics.

B. Data Preprocessing

To ensure high-quality data for deep learning training, the Sensors dataset was curated by selecting records from the MIMIC-III waveform database that simultaneously contain invasive ABP and fingertip PPG signals, and by incorporating subject age and gender information from the associated clinical records. Only recordings with a minimum duration of 15 minutes were retained. From these, 10-minute resting-state segments were extracted at 5-minute intervals to avoid data overlap. During signal preprocessing, low-quality segments were removed using flat segment and saturation peak detection analysis. Subsequently, the PPG signals were processed using a 0.5–8 Hz Butterworth bandpass filter and min-max normalization to mitigate the effects of noise and amplitude variations. Fig. 1 presents the overall procedure, starting from signal collection to the final estimation of blood pressure.

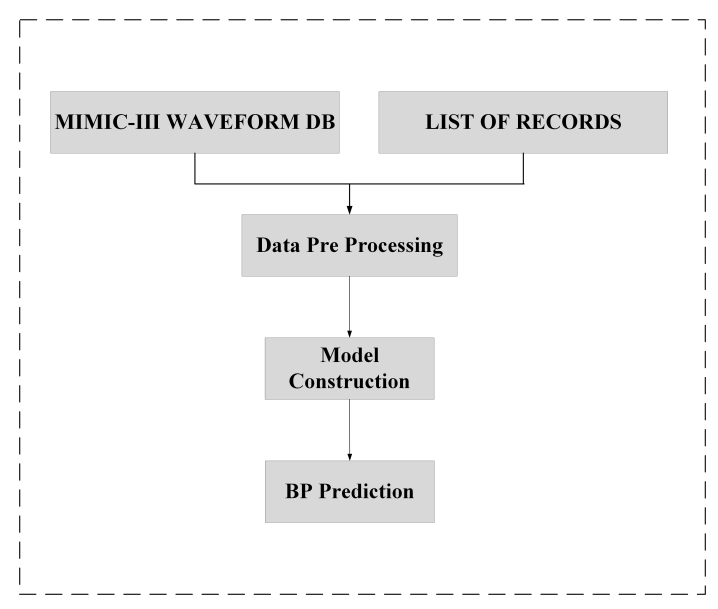


Fig. 1. Overview of the data handling procedure.

C. Model Architecture

To predict ABP waveforms from PPG signals, we developed and implemented a deep learning-based sequence-to-sequence modeling framework named Mamba-UNet. As shown in Fig. 2, the model adopts a symmetric encoder-decoder structure with skip connections to enable multi-level feature fusion. The architecture extensively integrates Mamba modules at various feature extraction stages to enhance temporal modeling capabilities.

In the encoder path, the network progressively extracts multi-scale temporal features through multiple layers of convolution and downsampling. At each scale, Mamba modules are embedded to leverage their state space modeling capacity, enabling the capture of critical patterns and long-term dependencies within the signal sequences. Unlike models that constrain temporal modeling to deeper layers, Mamba modules are incorporated throughout the network to capture both local and global temporal structures, enhancing robustness in modeling both periodic and transient dynamics.

The Mamba module is based on the SSM, which incorporates input-dependent dynamic parameters (e.g., Δ , B, C).

These allow the model to dynamically adapt the evolution of its internal state during sequence modeling.

In contrast to traditional linear time-invariant models, Mamba integrates optimizations such as kernel fusion and parallel scanning, achieving high memory efficiency and real-time inference capabilities while maintaining linear time complexity. This makes the architecture particularly well-suited for handling long physiological signal sequences.

In the decoder path, the model gradually upsamples the features and fuses them with corresponding encoder features via skip connections, thereby recovering the fine-grained structure of the ABP waveform. Ultimately, the network outputs an ABP waveform that is temporally aligned with the input PPG signal, enabling non-invasive and continuous blood pressure monitoring. The design of this model effectively combines the multi-scale feature integration strength of U-Net with the efficient temporal modeling power of Mamba, achieving a balance between detail restoration and global dynamic comprehension, and demonstrating superior performance in ABP waveform reconstruction.

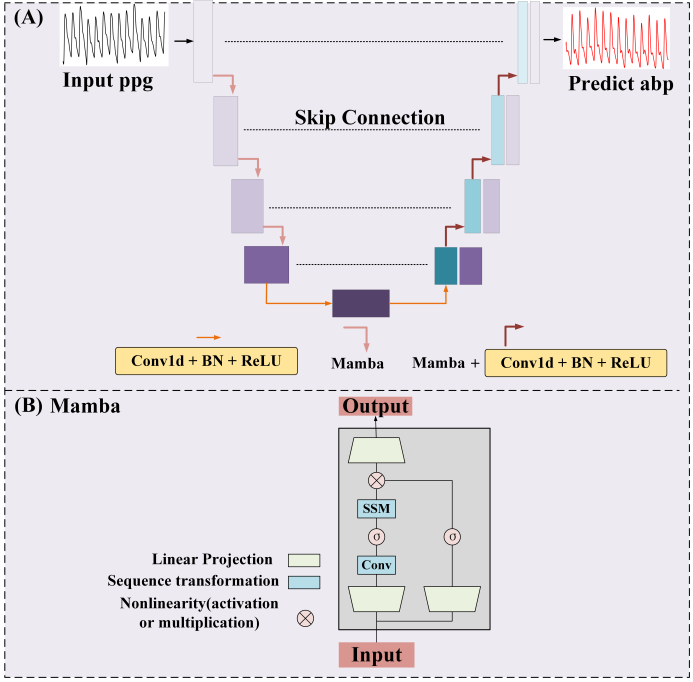


Fig. 2. Architecture of the PPG-to-ABP Prediction Model Based on Mamba and U-Net. (A) Overall Model Architecture. (B) Detailed Workflow of the Mamba Module(adapted from [14]).

D. Experimental Setup

To comprehensively evaluate the performance of the proposed model in the ABP estimation task, this study adopts a 10-fold cross-validation strategy to partition the dataset. Specifically, the dataset is evenly divided into 10 subsets. In each iteration, one subset is selected as the test set, one as the validation set, and the remaining eight subsets are used as the training set, cycling through all the subsets to ensure

that the model's generalization ability is fully validated across different subsets.

During training, the batch size is set to 64, the initial learning rate to 0.001, and the Adam optimizer performs the optimization. The training runs for 50 epochs. The model uses the mean squared error (MSE) as the objective function to minimize the error between the predicted and true blood pressure values. The performance evaluation metrics for blood pressure estimation include MAE and mean error (ME). These metrics are used to evaluate the model's average prediction deviation and systematic bias, respectively, providing a comprehensive reflection of the model's predictive capability across different individuals and waveform patterns.

III. RESULTS

Table II summarizes the blood pressure estimation performance of the proposed model on the Sensor dataset. The model achieves a MAE of 6.06 mmHg for DBP and 13.11 mmHg for SBP. Furthermore, it shows acceptable bias levels, with ME values of -0.91 mmHg for DBP and 1.89 mmHg for SBP.

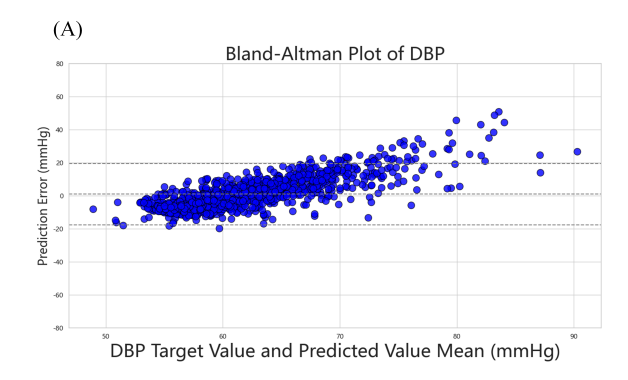
In addition, Table II presents the DBP and SBP estimation results of the proposed model in comparison with the British Hypertension Society (BHS) standard. For DBP, the model achieved a MAE of 6.06 mmHg and a ME of -0.91 mmHg, indicating a relatively low overall deviation and minimal systematic bias. According to the BHS grading criteria, 43.21% of DBP predictions fall within ± 5 mmHg, 78.3% within ± 10 mmHg, and 92.6% within ± 15 mmHg, meeting the threshold for Grade C performance. In contrast, the estimation performance for SBP is notably lower, with a higher MAE of 13.11 mmHg and an ME of 1.89 mmHg, suggesting both greater variability and a tendency to overestimate. Only 22.42% and 48.11% of SBP predictions fall within ± 5 mmHg and ± 10 mmHg, respectively, indicating a considerable gap from the requirements for higher BHS grades. Overall, the model demonstrates promising accuracy in DBP estimation, while further refinement is needed to improve SBP prediction.

TABLE II
EVALUATION OF OUR MODEL'S DBP AND SBP ESTIMATION
PERFORMANCE COMPARED WITH BHS STANDARDS.

Standard or Protocol	Metrics	DBP	SBP
Our results	MAE	6.06	13.11
Our results	ME	-0.91	1.89
BHS	≤ 5 mmHg (%)	43.21	22.42
	≤ 10 mmHg (%)	78.3	48.11
	≤ 15 mmHg (%)	92.6	63.57
	Grade	С	-

Fig. 3 and Fig. 4 show the Bland-Altman and correlation plots comparing the predicted and reference values of DBP and SBP. The Bland-Altman plot is used to assess the agreement between the predicted and reference values, with the dashed lines representing the 95% confidence interval (ME \pm 1.96 \times SDE). From the plot, it is evident that most of the estimation points for both SBP and DBP fall within the 95% limits, indicating that the model exhibits good bias control and system

consistency in its predictions. This suggests that the predicted values are generally in close agreement with the reference values. Furthermore, the correlation plot provides additional evidence supporting the reliability of the model's predictions, as it shows a strong linear relationship between the predicted and true values, further confirming the accuracy and robustness of the model.



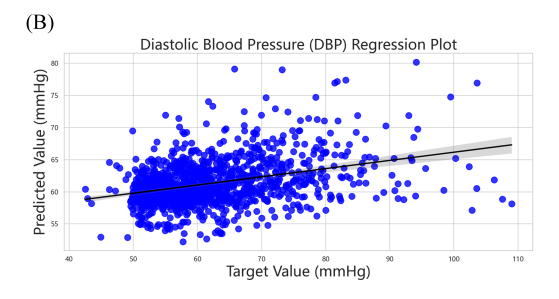
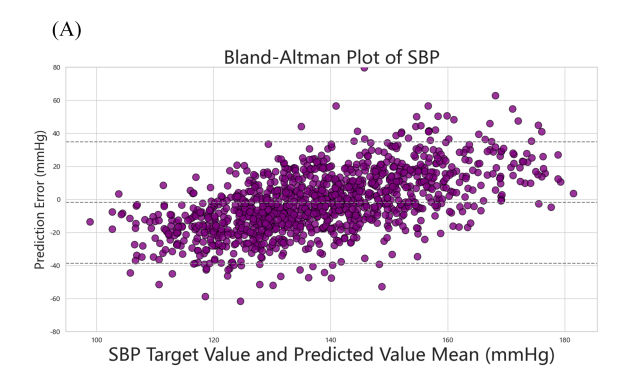


Fig. 3. Bland-Altman plot and linear regression plot between DBP estimated blood pressure values and reference blood pressure values.

To evaluate the performance of the employed model, we compared it with several representative blood pressure estimation methods based on machine learning and deep learning from existing research. In terms of deep learning methods, we implemented several classical networks that have shown strong performance in blood pressure estimation tasks, including MLP, ResNet, and U-Net. These models have been demonstrated in previous literature to have good potential for non-invasive blood pressure estimation. All comparison methods were evaluated using the same data splitting scheme, training, validation, and testing processes as those used for the employed model, ensuring fairness and consistency in the comparisons. As shown in Table III, the employed model outperforms these methods in several performance metrics, further validating its effectiveness and leading performance in blood pressure estimation tasks.

The results in the table indicate that the employed model performs relatively well in both SBP and DBP estimation. It achieves the lowest MAE among all models, with 13.11 for SBP and 6.06 for DBP, demonstrating a clear advantage in prediction accuracy. Although its ME for SBP is 1.89, suggesting a slight overestimation, the overall predictions are closer to the true values. For DBP, the ME is -0.91, indicating a slight underestimation, yet the error remains smaller than



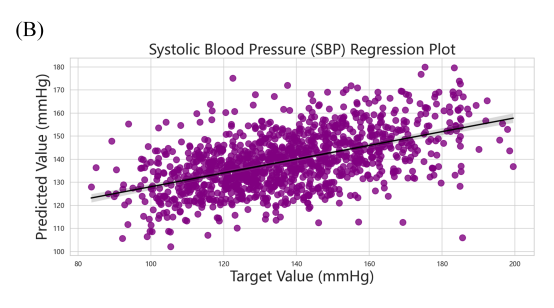


Fig. 4. Bland-Altman plot and linear regression plot between SBP estimated blood pressure values and reference blood pressure values.

TABLE III

COMPARISON OF DIFFERENT ALGORITHMS FOR SBP AND DBP
ESTIMATION PERFORMANCE.

Algorithm	SBP Estimation		DBP Estimation	
	MAE	ME	MAE	ME
MLP	16.05	-0.50	7.67	-0.19
ResNet	17.37	-1.21	8.42	-0.77
U-Net	15.23	-1.94	7.35	-0.52
Proposed	13.11	1.89	6.06	-0.91

that of the other models. In contrast, ResNet and U-Net exhibit moderate performance on both metrics, with noticeable prediction bias. MLP shows smaller bias but higher overall error. Overall, the model demonstrates superior robustness and accuracy in both SBP and DBP estimation tasks.

IV. CONCLUSION

This paper employed Mamba-UNet for PPG-based BP estimation. The encoder applied a MambaConvBlock to capture long-range temporal dependencies and vascular variability, while the decoder incorporated a hybrid Mamba-convolution module for accurate BP waveform reconstruction. A dynamic selection mechanism helps suppress motion artifacts, and hardware-aware design improves computational efficiency. Evaluated on the Sensors dataset (derived from MIMIC-III, with 1,131 ICU patient signal pairs), Mamba-UNet achieved a MAE of 6.06 mmHg for DBP and 13.11 mmHg for SBP, with low bias (ME: -0.91 for DBP, 1.89 for SBP). Compared to MLP, ResNet, and U-Net models, Mamba-UNet showed superior accuracy. However, SBP estimation still requires improvement to meet clinical standards. Nonetheless, Bland-Altman and correlation analyses confirmed strong

agreement between predicted and reference BP values, highlighting Mamba-UNet's potential for real-time, non-invasive BP monitoring. These results indicate that Mamba-UNet holds strong potential for deployment in wearable health monitoring devices, enabling continuous and comfortable non-invasive BP tracking in both clinical and home environments.

REFERENCES

- E. J. Benjamin, P. Muntner, A. Alonso, et al, "Heart Disease and Stroke Statistics-2019 Update: A Report From the American Heart Association," Circulation, vol. 139, no. 10, pp. e56–e528, 2019.
- [2] K. M. Sepiso and K. Annet, "Hypertensive heart disease: risk factors, complications and mechanisms," Frontiers in Cardiovascular Medicine, vol. 10, art. 1205475, 2023.
- [3] P Wu, Z Bai, P Xia, et al, "Wearable Continuous Blood Pressure Monitoring Based on Pulsatile Cycle Volume Adjustment Method," Tsinghua Science and Technology, vol. 30, no. 2, pp. 650-669, 2025.
- [4] R. Shriram, A. Wakankar, N. Daimiwal, et al, "Continuous cuffless blood pressure monitoring based on PTT," 2010 International Conference on Bioinformatics and Biomedical Technology, IEEE, pp. 51-55, 2010.
- [5] Zhang B, Wei Z, Ren J, et al, "An empirical study on predicting blood pressure using classification and regression trees," IEEE Access, vol. 6, pp. 21758-21768, 2018.
- [6] Zhang B, Ren H, Huang G, et al, "Predicting blood pressure from physiological index data using the SVR algorithm," BMC bioinformatics, vol. 20, pp. 1-15, 2019.
- [7] Zhang B, Ren J, Cheng Y, et al, "Health data driven on continuous blood pressure prediction based on gradient boosting decision tree algorithm," IEEE Access, vol. 7, pp. 32423-32433, 2019.
- [8] H. M. Jiun-Ruey, MPH, B. M. Gabrielle, et al, "Validating cuffless continuous blood pressure monitoring devices," Cardiovascular Digital Health Journal, vol. 4, no. 1, pp. 9-20, 2023.
- [9] M. Elgendi, R. Fletcher, Y. Liang, et al, "The use of photoplethysmography for assessing hypertension," NPJ digital medicine, vol. 2, no. 1, art. 60, 2019.
- [10] G. F. S. Silva, T. P. Fagundes, B. C. Teixeira, et al, "Machine learning for hypertension prediction: a systematic review," Current hypertension reports, vol. 24, no. 11, pp. 523-533, 2022.
- [11] J. Esmaelpoor, M. H. Moradi, A. Kadkhodamohammadi, "A multistage deep neural network model for blood pressure estimation using photoplethysmogram signals," Computers in Biology and Medicine, vol. 120, art. 103719, 2020.
- [12] M. Sadrawi, Y. T. Lin, C. H. Lin, et al, "Genetic deep convolutional autoencoder applied for generative continuous arterial blood pressure via photo plethysmography," Sensors, vol. 20, no. 14, art. 3829, 2020.
- [13] G. Ślapničar, N. Mlakar, M. Luštrek, "Blood pressure estimation from photoplethysmogram using a spectro-temporal deep neural network," Sensors, vol. 19, no. 15, art. 3420, 2019.
- [14] A. Gu and T. Dao, "Mamba: Linear-time sequence modeling with selective state spaces," 2023, arxiv:2312.00752. [Online]. Available: https://doi.org/10.48550/arXiv.2312.00752
- [15] N. Aguirre, E. Grall-Maës, L. J. Cymberknop, et al, "Blood pressure morphology assessment from photoplethysmogram and demographic information using deep learning with attention mechanism," Sensors, vol. 21, no. 6, art. 2167, 2021.